PII: S0032-3861(97)10263-4

Polymer Vol. 39 No. 22, pp. 5431–5439, 1998
© 1998 Elsevier Science Ltd.
All rights reserved
0032-3861/98/$ - see front matter

PVAc phase precipitation in vinyl ester and polyester resins

Wayne D. Cook[a,b,*], **Marcus D. Zipper**[a,b,†] **and Andrew C. -H. Chung**[a,b]
[a]*Department of Materials Engineering Monash University, Notting Hill, Melbourne, Victoria, Australia 3168*
[b]*CRC for Polymers, 32 Business Park Drive, Nottinghill, Melbourne, Victoria, Australia 3168*
(Received 25 July 1997; accepted 29 September 1997)

The precipitation of poly(vinyl acetate) (PVAc) during the cure of vinyl ester resins and unsaturated polyester resins has been studied. The rate of polymerization, measured by differential scanning calorimetry, was virtually independent of the PVAc additive and the activation energy (at the peak rate) was approximately constant at 70 kJ mol^{-1}, in agreement with theoretical estimates. A turbidity technique was found to be useful in studying the phase precipitation process. The start of phase precipitation was found to be strongly correlated with the start of the polymerization process and the end of the induction stage. The induction stage was shown to be caused by radical consumption by the inhibitor in the resin. The onset time for phase precipitation was shown to be proportional to inhibitor concentration and reciprocally related to the initiator concentration. The activation energy for the onset of phase precipitation, calculated by isothermal or scanning techniques, was close to the activation energy for initiator decomposition as predicted. Dynamic mechanical thermal analysis confirmed the occurrence of phase separation in the cured resins and suggested that a co-continuous morphology was developed around 5 wt% PVAc. © 1998 Elsevier Science Ltd. All rights reserved.

(Keywords: polyester resin; vinyl ester resin; low profile additives)

INTRODUCTION

Styrenated unsaturated polyesters are a widely used matrix in sheet moulding and bulk moulding compounds in the aeronautical and automotive industries. As with most unfilled thermosetting systems, the large polymerization shrinkage (7–10%) during cure is a major problem leading to poor surface quality and lack of dimensional stability[1,2]. Several techniques (such as in-mould coating, inclusion of 5–20 wt% low profile additives (LPAs) and finishing operations) have been developed to alleviate these problems[1–3].

Many different LPAs have been investigated with varying success, some of the more common being poly(vinyl acetate) (PVAc), poly(styrene) and poly(methyl methacrylate)[1,2]. Many LPAs are soluble in the uncured polyester resin but undergo phase separation at some stage during cure[1,2]. The exact mechanism of shrinkage reduction by LPAs is still a topic of debate and many publications[1–10] have been devoted to its understanding.

Reaction-induced phase precipitation in step growth polymerization is a result of the effect of network formation on the free energy of the system[11]—as the reaction proceeds, branching leads to a rapid increase in molecular weight and a decrease in entropy of the system. This reduction in entropy causes the free energy of mixing to be less favourable and, as a result, phase separation may ensue. In chain-growth network formation, such as occurs with the copolymerization of vinyl and multivinyl monomers, the situation is complicated as there is considerable evidence for heterogeneity in the development of the network[12,13].

Network formation in polyester and vinyl ester resins is even more complex, due to the presence of two different reactive unsaturation sites—the vinyl group on the mobile styrene monomer and the unsaturation in the less mobile and readily crosslinked polyester or dimethacrylate resin. Lee and coworkers[14,15] have extended the concept of heterogeneity in chain-growth polymerized networks by proposing the formation of microgels during the polymerization of unsaturated polyester resins, and Liu *et al.*[16] have recently reported gel permeation chromatography (g.p.c.) evidence for these particles. The microgel particles are believed to develop by hyper-branching of the polyester molecules during the copolymerization process causing spherical structures to develop with unsaturation sites trapped inside. Styrene monomer is free to diffuse into the internal regions of these growing microgel particles and further copolymerize[14,15]. As the reaction proceeds, the microgels can agglomerate to form larger structures which interpenetrate the liquid phase leading to macroscopic gelation[14,15].

When an additional component, such as a LPA, is incorporated into the system, the relative differences in polarity of styrene, unsaturated polyester and the LPA further complicate the issue. Hsu *et al.*[8] have shown by scanning electron microscopy (SEM) that, at low degrees of conversion, a nodular structure of spherical particles (diameter *ca.* 1 μm) develops in LPA systems (with PVAc), whereas the unfilled resin showed only a coarse, flake-like appearance. These differences in microstructure may reveal how the presence of the PVAc enhances the propensity of the chain growth crosslinking process for heterogeneity. According to the most commonly accepted model for phase precipitation in LPA systems[3–10], the formation of high molecular weight microgel particles and

---

[*] To whom correspondence should be addressed
[†] Current address: Huntsman Chemical Company Australia Pty Ltd, Sommerville Road, PO Box 62, West Footscray, Victoria, Australia 3012

the concomitant decrease in entropy causes the system to begin phase separation into a crosslinked polyester rich phase and a PVAc/styrene rich phase. As the reaction proceeds and the density of microgel increases, the particles coalesce to form a continuous phase causing the material to show the macroscopic characteristics of gelation. Further reaction may lead to the development of a co-continuous structure of PVAc and styrene-unsaturated polyester or a polyester resin matrix with dispersed PVAc particles, depending on compositional factors. In some cases the morphology is even more complex—Bucknall *et al.*[17] have observed PVAc panicles with polyester network sub-inclusions. It is interesting to note that although low levels of PVAc have been found[5] to toughen unsaturated polyesters, higher levels which resulted in a change in morphology to a co-continuous structure had impaired properties.

The development of a two phase structure is considered essential for low profile action. Several studies[2,3] have shown that the thermal and polymerization shrinkage is offset by microcracking at the interface and cavitation within the LPA phase approximately mid-way through the reaction[10]. However, Suspène *et al.*[10] have concluded that although the phase precipitation model qualitatively describes the mechanism of LPA action, the actual structure and morphology which develops is controlled by the specific kinetics of polymerization and phase separation. In addition, Suspène *et al.*[10] note that the exact correlation between the extent of microvoid formation and volume control is still to be determined. Related to this, Kinkelaar *et al.*[3] have also concluded that while the morphology of the dispersed phase affects shrinkage, it does not completely determine the reduction in shrinkage.

Thus the mechanism and kinetics of phase precipitation of LPAs, their influence on thermoset morphology and their exact function are matters which are still uncertain and require further research. In the present work, we extend a previous study[18] of the curing behaviour of vinyl ester resins by investigating the kinetics of precipitation of PVAc from vinyl ester and polyester resins. To our knowledge, the present study is the first to investigate this process in vinyl ester resins.

EXPERIMENTAL

Two thermosetting systems, supplied by the Huntsman Chemical Company, Australia, were used in this study. The vinyl ester resin, HETRON® 922 (a registered trademark of Occidental Chemical Corporate), contains approximately 45 wt% styrene and 55 wt% of a dimethacrylate based on an oligomerized diglycidyl ether of bisphenol-A. The molecular weight of the dimethacrylate is approximately 1000 and its generic structure is shown in *Figure 1*. When $n = 1$ in *Figure 1*, the resin is known as bisGMA or bisphenol-A di(glycidyl methacrylate). The unsaturated polyester resin used (*Figure 1*), AROPOL™ 4021P (a registered trademark of Ashland Oil Inc.), is a pre-promoted orthophthalate based product containing approximately 35 wt% styrene. The levels of hydroquinone (HQ) stabilizer in the polyester and vinyl ester resins were reported to be 0.002 and 0.035 wt%, respectively. Curing was performed at elevated temperature with typically 1 wt% cumene hydroperoxide (CHP), a common initiator for polyester systems, also provided by the Huntsman Chemical Company, Australia. The HQ and CHP levels are expressed as a percentage of the mass of resin.

PVAc (Vinnapas B60, Wacker Chemie) with a weight-average molecular weight (M_w) of 74,000 g mol^{-1} was used for all differential scanning calorimetry (d.s.c.), optical microscopy studies and dynamic mechanical thermal

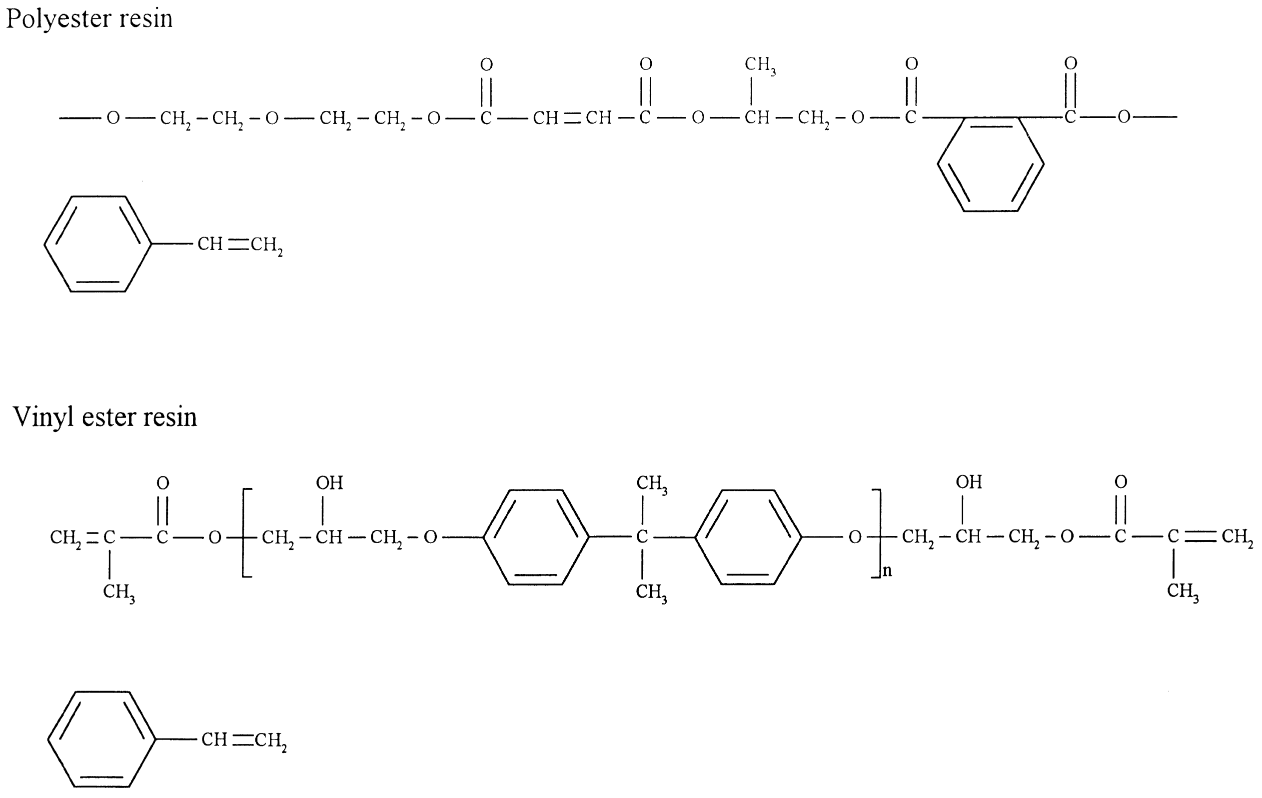

Figure 1 Structures of monomers used

analysis (DMTA) measurements. Solutions of the PVAc were prepared in each resin and after complete dissolution, the initiator was added.

The curing kinetics were monitored in duplicate on a Perkin Elmer DSC-7, calibrated with indium and zinc standards. Resin samples with a sample mass in the range of 5–10 mg were sealed in aluminium pans and studied in dynamic mode at scan rates ranging from 1 to 20°C $\min^{-1}$. In some cases, the Perkin Elmer Intracooler was used for sub-ambient runs.

The phase precipitation of the PVAc from the thermosetting resins was monitored in duplicate by a turbidity measurement technique using a Mettler ZU FP82 photomonitor attached to a Mettler FP80 microscope hot-stage and Olympus BHSP microscope. A disc of the resin was pressed between a glass slide and a cover-slip and this assembly was placed inside the hot-stage. The thickness of the resin disc was varied from 0.14 to 1 mm, however 1 mm was standard. Since varying samples had different light transmission, all data was normalized to the initial transmission of the resin. The relative light intensity was either monitored as a function of time (for isothermal experiments) or temperature (for dynamic experiments) and the data were acquired at one datum per second by a personal computer. Dynamic scans were made from 25 to 200°C at various heating rates (1–20°C $\min^{-1}$). By inserting a thermocouple into the curing solution during isothermal cure, the equilibration time was estimated to be less than 60 s. For dynamic experiments, the thermal lag was estimated to be 1°C at 5°C $\min^{-1}$ and 5°C at 20°C $\min^{-1}$. The data was not corrected for these thermal lags.

DMTA of the blends was performed with double cantilever geometry using a Rheometrics Mk II DMTA operated at 1 Hz and scanned at 2°C $\min^{-1}$. Samples for the DMTA, 2 mm thick and 5.5 mm wide and effective span of 32 mm, were prepared by curing in aluminium moulds. The polyester resin was cured at 80°C for 270 min and then postcured for 60 min at 100°C, while the vinyl ester resin was cured at 100°C for 180 min and then 130°C for 120 min.

RESULTS AND DISCUSSION

Dynamic curing behaviour

The rate of free-radical polymerization (d[M]/d*t*) can be written as[19]:

$$-\frac{\mathrm{d}[M]}{\mathrm{d}t} = k_\mathrm{p}\left(\frac{fR_\mathrm{i}}{k_\mathrm{t}}\right)^{1/2}[M] \qquad (1)$$

where [M] is the concentration of vinyl groups, k_p and k_t are the rate constants for propagation and termination, f is the initiation efficiency and R_i is the rate of initiation. For uncatalysed decomposition of a hydroperoxide (ROOH) to alkoxy (RO·) and hydroxy (·OH) radicals, the reaction process can be written as[19]:

$$\mathrm{ROOH} \xrightarrow{k_d} \mathrm{RO\cdot} + \mathrm{\cdot OH} \qquad (2)$$

and the rate of radical production is:

$$R_\mathrm{i} = k_\mathrm{d}[\mathrm{ROOH}] \qquad (3)$$

where k_d is the rate constant for the production of free radicals and [ROOH] is the concentrations of peroxide. For catalysed systems, the rate expression would also include the concentration of the reducer, but for our purposes the form of equation (2) will suffice.

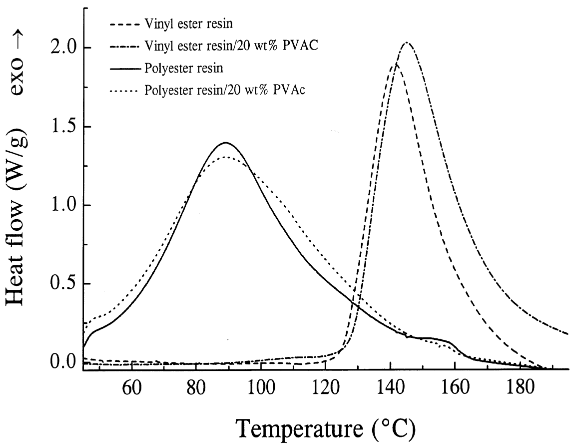

Figure 2 Dynamic d.s.c. traces at 10°C $\min^{-1}$ for the cure of the polyester and vinyl ester resin with 1 wt% CHP and containing 0 or 20 wt% PVAc

To improve storage life and for ease of application, resin systems contain varying levels of inhibitor (*X*) whose purpose is to consume adventitious radicals (R·) during storage and to provide an induction time in the early stages as shown by the reaction:

$$\mathrm{R\cdot} + \mathrm{X} \xrightarrow{k_\mathrm{x}} \mathrm{RX\cdot} \qquad (4)$$

where RX· is an inactive radical, and k_x is the rate of inhibition.

Figure 2 shows the scanning d.s.c. traces for polyester and vinyl ester resins with and without PVAc. In the early stages of the scanning d.s.c. run, little heat is evolved but as the temperature rises, the curing reaction accelerates and heat is generated at a steadily increasing rate. The increase in the rate of heat generation is due to changes in the rates of initiator decomposition, monomer propagation and radical termination with temperature and conversion. After the induction stage, the concentrations of initiator and monomer are relatively constant, so that the rate of polymerization depends primarily on k_p, k_t and R_i. As the temperature rises further, the concentration of monomer and possibly initiator begins to be depleted and the rate of polymerization passes through a maximum and finally results in cessation of the reaction as illustrated in *Figure 2.*

The data shown in *Figure 2* also indicate that the vinyl ester resin requires higher temperatures to cure and thus polymerizes at a lower rate in comparison with the polyester resin. This is probably due to the presence of a co-catalyst (promoter) in the polyester resin which produces an acceleration in the rate of hydroperoxide decomposition. In addition, the higher level of inhibitor in the vinyl ester resin and differences in the reactivity of styrene with the fumarate and methacrylate unsaturation might also play a role in this behaviour.

The presence of the PVAc phase does not appear to have any significant influence on the polymerization process as indicated by the data in *Figure 2.* This observation is confirmed in *Table 1,* which shows that the heat of polymerization for the polyester and vinyl ester resins are virtually independent on the level of PVAc in agreement with the results of Ruffier *et al.*[9]. These observations contrast with those of Lem and Han[20] where the addition of PVAc was reported to decrease the heat of polymerization.

Due to the temperature sensitivity of the various reaction processes, the heat flow curve is affected by scanning rate.

Table 1 Heat of polymerization and activation energy obtained by scanning d.s.c. measurements. The resins contained 1 wt% cumene hydroperoxide

Resin	PVAc (wt%)	ΔH_p (J per g of resin)	E_a (kJ mol^{-1})^a from peak	E_a (kJ mol^{-1})^a from onset
Polyester	0	354	69 ± 5	
Polyester	10	324^b, 366^b, 366^b, 350^b	68 ± 5	105 ± 7
Polyester	20	345		
Vinyl ester	0	389		
Vinyl ester	10	394^b, 378^b, 342^b, 380^b	73 ± 2	100 ± 4
Vinyl ester	20	388		

[a] Average ± standard deviation from the fitted line

[b] Determined at scan rates of 2, 5, 10 and 20°C min^{-1}. All other values obtained at scan rates at 10°C min^{-1}

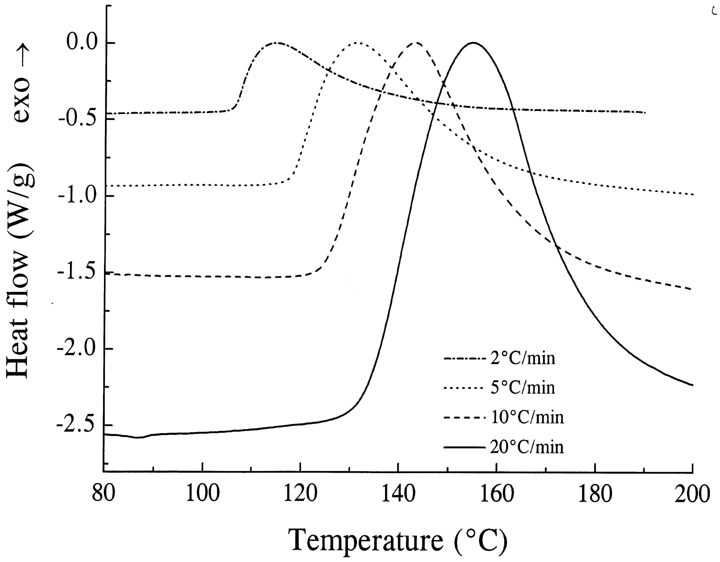

Figure 3 Effect of scan rate on the heat flow traces during cure of vinyl ester resin with 1 wt% CHP and containing 10 wt% PVAc

The influence of scan rate on the d.s.c. curves is illustrated in *Figure 3* for the cure of the polyester resin containing 10 wt% PVAc. Similar results were obtained for the vinyl ester resin. As the scan rate is increased, the temperature and magnitude of the exotherm peak is raised but the heat of polymerization is virtually independent of scan rate (see *Table 1*). The activation energy (E_a) of the polymerization process was calculated from the dependence of peak temperature on scan rate[21,22] and these values are also tabulated in *Table 1*. The activation energy (E_a) does not appear to be influenced by the presence of PVAc and is similar for the vinyl ester resin and the polyester resin. From equation (1), the activation energy for the polymerization process can be broken up into the components for decomposition of the initiator, propagation and termination:

$$E_a = E_{a(\text{propagation})} + 1/2E_{a(\text{decomposition})} - 1/2E_{a(\text{termination})} \tag{5}$$

Assuming that the activation energy for decomposition of the cumene hydroperoxide is unaffected by the promoter in the polyester resin, $E_{a\ (\text{decomposition})}$ is 101 kJ mol^{-1} in styrene[23] (and varies from 99 to 122 kJ mol^{-1} in other media[24]). Since the majority of the monomer unsaturation is in the form of styrene, $E_{a\ (\text{propagation})}$ can be assumed to be that for the polymerization of styrene[19], 26 kJ mol^{-1}. The activation energy for termination is a poorly defined quantity because the initiation efficiency and the termination mechanism change through the reaction[19,25,26]. In the early stages of the reaction, E_a for termination of styrene radicals is 8 kJ mol^{-1} (see Ref. 19), but when the reaction is controlled by reaction diffusion, the termination rate is determined by the propagation rate[25,26] and so $E_{a(\text{termination})}$ is equal to $E_{a(\text{propagation})}$. Thus the overall E_a is predicted to lie between 64 and 73 kJ mol^{-1} which is in good agreement with the experimental observations (*Table 1*).

If the inhibitor is efficient and one can ignore the loss of radicals by bimolecular termination, then radicals produced by the mechanism in equation (2) will be almost immediately consumed by inhibitor (equation (4)) and a steady state concentration of radicals will exist. Thus the rate of change in radical concentration will be:

$$d[R\cdot]/dt = k_d[\text{ROOH}] - k_x[R\cdot][X] = 0 \tag{6}$$

and so:

$$[R\cdot] = k_d[\text{ROOH}]/k_x[X] \tag{7}$$

Thus the rate of loss of inhibitor, as shown by the reaction in equation (4), is given by[19,27]:

$$\begin{aligned} -d[X]/dt &= k_x[R\cdot][X] \qquad (8) \\ &= k_d[\text{ROOH}] \end{aligned}$$

When the inhibitor is finally consumed, the polymerization reaction can commence. Thus the 'onset' of polymerization, as shown in the initial stages of the dynamic d.s.c. curves in *Figure 3*, is controlled by this inhibition reaction. From equation (8), the rate of consumption of inhibitor is determined by k_d and [ROOH] so the duration of the induction

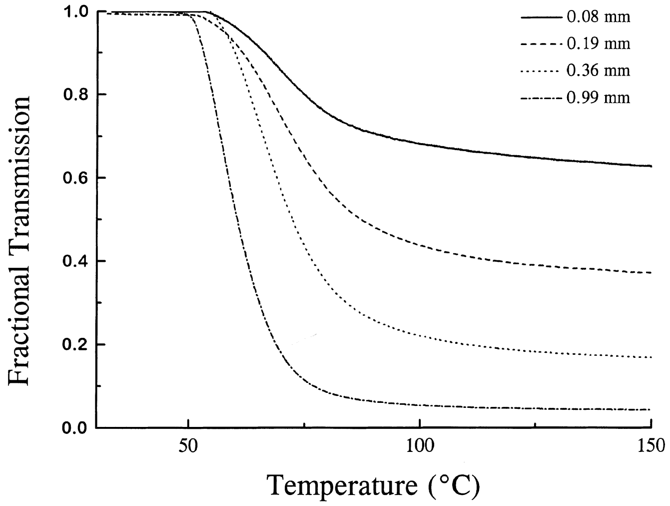

Figure 4 Effect of film thickness on dynamic turbidity curves for the polyester resin with 1 wt% CHP and 10 wt% PVAc, scanned at 5°C min^{-1}. The initial transmissions have been normalized to unity

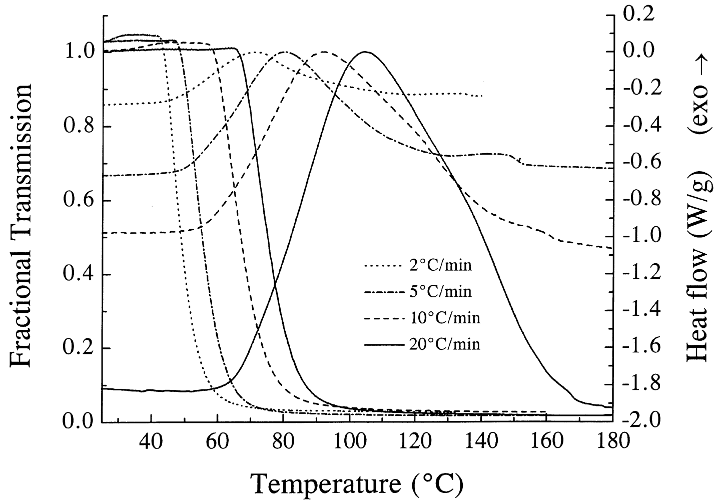

Figure 5 Correlation of dynamic turbidity traces and dynamic d.s.c. traces for the polyester resin with 1 wt% CHP and 10 wt% PVAc

period depends on the rate of CHP decomposition (which varies with heating rate) and the CHP and HQ concentrations (which are constant). In the same way that the scan rate dependence of the peak temperature can yield the activation energy for the polymerization process, the temperature at the 'onset' of polymerization can be analysed by the scan rate method[21,22] to give the activation energy for the rate process operative in this region of the d.s.c. trace. Because the rate of loss of inhibitor is determined by k_d, the E_a thus calculated is the activation energy for the hydroperoxide decomposition. Thus the E_a values from dynamic d.s.c. studies and listed in *Table 1* are close to the literature value for the decomposition of cumene hydroperoxide in styrene (101 kJ mol^{-1})[23].

Turbidity

Figure 4 shows typical dynamic turbidity curves for the polyester resin with 10 wt% PVAc. Initially the light intensity is approximately constant but as the temperature increases, the intensity suddenly plummets and then appears to level out. Although the final transmission varies with thickness, the initial reduction in transmission occurs at a constant temperature (at 53 ± 2°C for the data in *Figure 4*). This transition temperature was also found to be relatively constant (to within ±2°C) and independent of the PVAc concentration. However, the final degree of turbidity during cure depended on the amount of PVAc in the resin. Uninitiated samples did not show these turbidity changes during temperature scanning until much higher temperatures were reached. This confirms that the change in light transmission is associated with the phase precipitation of the PVAc during the cure process and is not caused when the system reaches the lower critical solution temperature of the unpolymerized solution. Since the refractive indices of the uncured unsaturated polyester and vinyl ester resins were 1.533 and 1.5707 at 23°C, which differ considerably from that of 1.467 for PVAc, it can be assumed that once phase separation commences, the material starts to loose clarity.

As shown in *Figure 5*, the dynamic turbidity traces for the polyester resin exhibit a strong dependency on scan rate which is similar to the scan rate dependency of the corresponding d.s.c. results. Similar behaviour was also observed for the vinyl ester resin system. In addition, *Figure 5* illustrates that a good correlation exists between the temperature where polymerization rate becomes

Table 2 Activation energies for the onset of phase precipitation as obtained by dynamic and isothermal turbidity measurements. The resins contained 10 wt% PVAc and 1 wt% cumene hydroperoxide

Resin system	Added inhibitor (wt%)	E_a (kJ mol^{-1})^a from scanning	E_a (kJ mol^{-1})^a from isothermal
Polyester	0		90 ± 4
Polyester	0	76 ± 2	
Polyester	0.005		78 ± 9
Polyester	0.01		103 ± 4
Polyester	0.015		102 ± 1
Polyester	0.02		105 ± 9
Vinyl ester	0		88 ± 3
Vinyl ester	0	85 ± 5	

[a] Average ± standard deviation from the fitted line

noticeable (as measured by d.s.c.) and the onset of the PVAc precipitation in the dynamic turbidity results. This result is in good agreement with the work of Hsu *et al.*[8] and Suspène *et al.*[10] which showed major changes in light transmission just prior to significant variations in the degree of cure. A similar correlation was also observed for the vinyl ester resins, however the onset of precipitation occurred at a temperature *ca.* 10°C above the observable start of polymerization. A related anomaly is also evident in the data of Hsu *et al.*[8]. It would appear that the discrepancy in temperature between the start of cure and the onset of phase precipitation is due to the difference in oxygen availability in the d.s.c. and turbidity samples. It is known[19,28] that phenolic stabilizers and oxygen have a synergistic effect in inhibiting free radical polymerization and prolonging the induction period. In the d.s.c. experiment, there is an oxygen reservoir in the air sealed in the d.s.c. pan which is capable of retarding the polymerization. In contrast, the larger turbidity sample is sealed between glass slides and is effectively separated from the atmosphere so that the induction period is only influenced by the concentration of oxygen dissolved in the resin. This discrepancy between the d.s.c. and turbidity results was not observed for the polyester resin system because it contained a much lower concentration of phenol-based inhibitor than in the vinyl ester resin system, thus lessening the synergistic effect.

The dependence of the onset of phase precipitation on the scan rate, shown in *Figure 5*, can also be analysed by the scanning method[21,22], giving an activation energy, and these values are listed in *Table 2*. If it is assumed that the onset of turbidity occurs when most of the inhibitor is consumed, i.e. at virtually zero conversion, then the activation energy calculated in this way is that for the rate process operative up to that time, *i.e.* the E_a value for the rate constant k_d for hydroperoxide decomposition. However, if a small amount of polymerization has occurred prior to the point of phase precipitation, then the calculated E_a would be a mixture of the activation energy for hydroperoxide decomposition and the overall polymerization process. The E_a values from dynamic turbidity studies are listed in *Table 2* and are midway between that found for the hydroperoxide decomposition (*ca.* 100 kJ mol^{-1}) and the polymerization process (*ca.* 70 kJ mol^{-1}).

Figure 6 shows isothermal turbidity curves as a function of cure temperature for the polyester resin. Similar data was obtained for the vinyl ester resin. With increased temperature, the onset time for phase precipitation decreases due to the acceleration of the hydroperoxide decomposition. For an isothermal polymerization and assuming that the initiator is not significantly depleted, equation (8) shows that the radical concentration will decrease with time, according to Refs [19,27,29]:

$$[X] = [X]_o - k_d[\mathrm{ROOH}]t \qquad (9)$$

where $[X]_o$ is the initial concentration of inhibitor. For active scavengers, the polymerization is effectively delayed until [X] approaches zero[19,27,30]. Therefore, from equation (9), the polymerization induction time is given by:

$$t = [X]_o/k_d[\mathrm{ROOH}] \qquad (10)$$

If phase precipitation is considered to occur shortly after the start of polymerization, the reciprocal of the onset time of phase precipitation can be used as a measure of the hydroperoxide decomposition rate and so an Arrhenius plot will yield the activation energy for this reaction. The E_as calculated from isothermal experiments similar to that shown in *Figure 6* are listed in *Table 2* for the polyester and vinyl ester resins. In many cases the isothermal E_a values are close to the value for CHP decomposition.

Equation (10) also predicts that the onset time will increase with raised inhibitor levels and will be reduced when the peroxide concentration is raised. This prediction is confirmed in *Figure 7* where the changes in turbidity are retarded or accelerated as the HQ and CHP levels are varied. In *Figure 8* the phase precipitation onset time for the

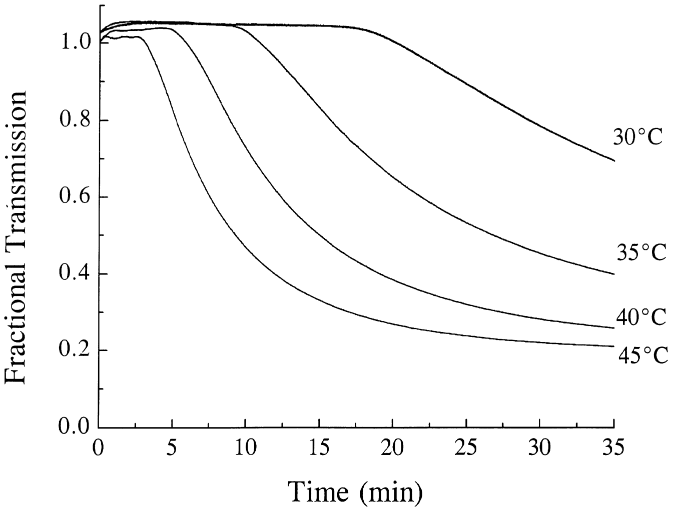

Figure 6 Isothermal turbidity scan at various temperatures for polyester resin with 1 wt% CHP and 10 wt% PVAc

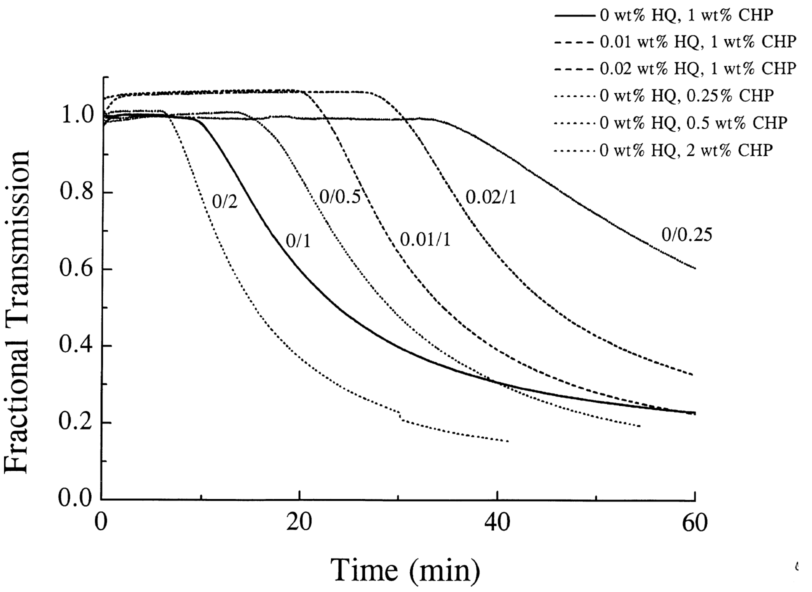

Figure 7 Isothermal turbidity scan at 35°C for polyester resin with 10 wt% PVAc and varying levels of HQ (dotted curves) and CHP (dashed curves). The concentrations of inhibitor and initiator (based on the mass of polyester resin) are printed adjacent to each curve as the ratio of wt% HQ added to CHP

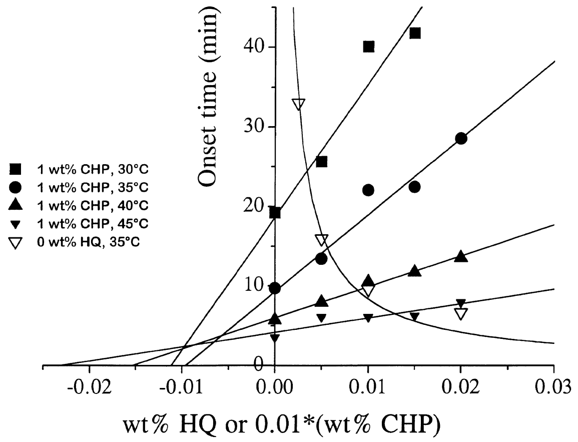

Figure 8 Isothermal turbidity onset time *versus* level of additional HQ inhibitor (at 1 wt% CHP, filled symbols) or CHP initiator (at 0 wt% additional HQ, open symbols) added to the polyester resin containing 10 wt% PVAc. The lines are fits to equation (10)

polyester resin is plotted *versus* the concentrations of added CHP initiator or hydroquinone inhibitor, according to equation (10). The data related to varying CHP concentration are reasonably well fitted by the hyperbolic least-square fit in accordance with equation (10). When additional HQ was added, the onset time is well fitted by linear regressions, as predicted by equation (10). Theoretically, the initial concentration of hydroquinone in the resin ($[X]_0$), is given by the X-axis intercept, however this value is not constant and is larger than the 0.002 wt% claimed by the manufacturer.

DMTA

Figures 9 and *10* show the temperature dependence of tanδ and storage modulus for the fully cured polyester and vinyl ester resins containing varying amounts of PVAc. For both thermosets, a relaxation is observed as a maximum in tanδ and a step in the modulus curve at *ca.* 40°C which is slightly higher than the T_g of 33°C at 1 Hz for PVAc[31]. Similar results have been observed by others[2,5]. As the level of PVAc is increased, the lower temperature tanδ peak increases slightly in temperature and increases in magnitude due to the increased fraction of a PVAc phase. The glass transition of the network is observed at a temperature near 120°C which shows some variation with PVAc content, but this does not appear to be systematic. It is interesting to note that the modulus in the rubbery region for both the polyester and the vinyl ester resins shows a substantial drop at PVAc levels higher than 5 wt%—this is more clearly illustrated in *Figure 11*. For a single phase polymer, the rubbery modulus

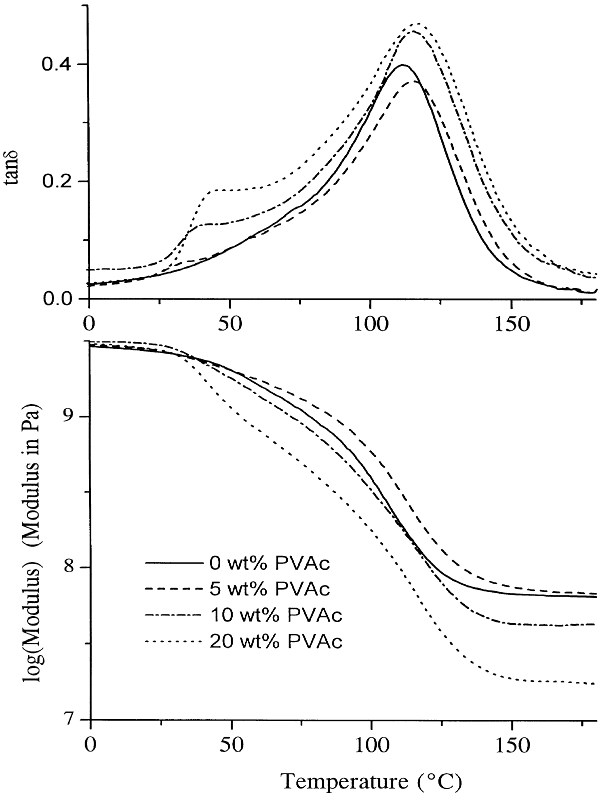

Figure 9 Flexural storage modulus and tanδ *versus* temperature for polyester resin with 0, 5, 10 and 20 wt% PVAc

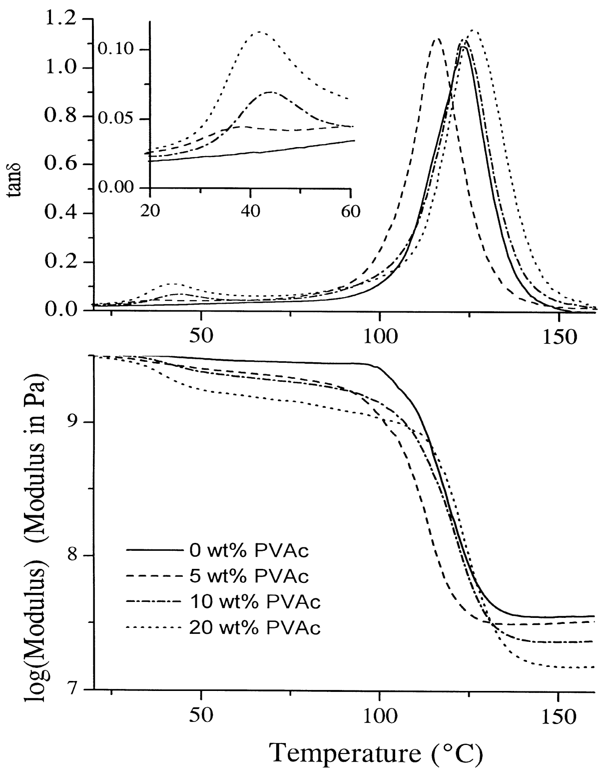

Figure 10 Flexural storage modulus and tan δ *versus* temperature for vinyl ester resin with 0, 5, 10 and 20 wt% PVAc

is proportional to the concentration of elastic network strands and hence crosslinks in the network structure[32]. The three-fold reduction in the rubbery modulus, shown in *Figure 11*, cannot be simply explained by the volume of the matrix occupied by the soft (above 50°C) PVAc particles but may be interpreted in terms of phase morphology. At low levels of additive, the PVAc phase may be assumed to be dispersed throughout the matrix and so the rubbery modulus is approximately that of the network phase alone. However, at sufficiently high concentrations the PVAc phase would be expected to become continuous with the network phase, thus reducing the connectivity of the thermoset phase through the sample and thus lowering the modulus. From *Figure 11*, it would appear that this occurs around 5 wt%. This level might appear low for the formation of a co-continuous structure. However, it has been suggested[8,10] that during cure, the PVAc is pushed to the surface of the growing microgel particle which reduces the tendency of the polyester gel particles to coalesce thus enhancing the formation of a continuous PVAc phase interpenetrating the network phase. Bucknall *et al.*[5] have also observed co-continuity in cured polyester resins with PVAc levels around 5 wt%. It is interesting to note that in the precipitation of PVAc from step-growth polymerized epoxy resins, co-continuous morphology has also been reported[17] to occur around 10 wt%.

CONCLUSIONS

Scanning d.s.c. studies have shown that the curing behaviour of either the polyester or vinyl ester resin is virtually unaffected by the presence of the PVAc or its phase precipitation. Similarly the activation energy measured at the maximum polymerization rate was independent of the PVAc level and was close to that predicted for cumene hydroperoxide initiated free radical polymerization.

A simple turbidity method was found to be useful for monitoring the phase precipitation process in isothermal as well as dynamic curing experiments. The observed correlation between the start of curing and the start of phase precipitation reinforces the important role that inhibition plays in determining the kinetics of phase precipitation. As a result, the activation energy for the onset of phase separation was close to the E_a for decomposition of the initiator. The onset of polymerization and thus phase precipitation was also controlled by the concentration of initiator and inhibitor as described by a simple inhibition model.

The dynamic mechanical properties of cured PVAc/resin blends clearly revealed two phases, corresponding to the PVAc and thermosetting resin. The modulus in the rubbery region decreased abruptly as the PVAC concentration approached 5 wt% PVAc additive, suggesting that a

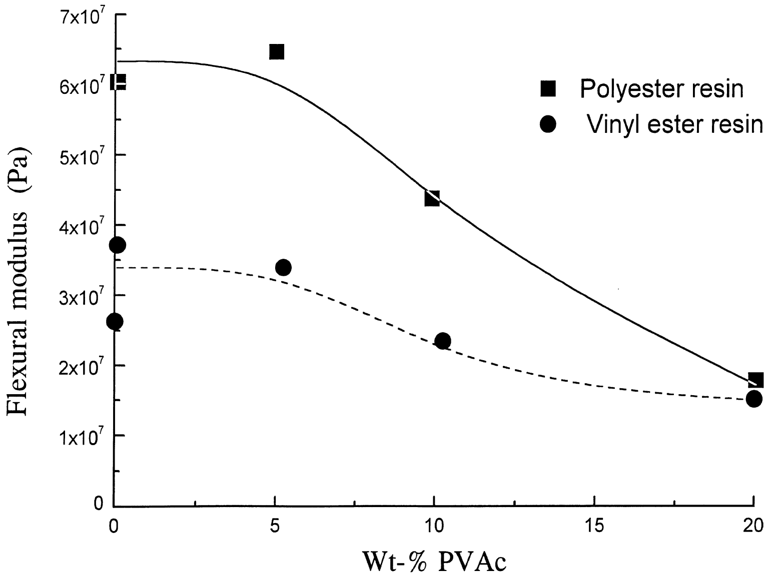

Figure 11 Flexural storage modulus in the rubbery region (determined at 160°C from the data in *Figures 9 and 10*) *versus* wt% PVAc for the vinyl ester and polyester resin

co-continuous structure had developed. This behaviour was interpreted in terms of the microgel model for the development of the network.

ACKNOWLEDGEMENTS

The authors would like to thank Dr Graham Durrant (Huntsman Chemicals) for supplying the polyester and vinyl ester resins and for helpful discussions, Mr Chris Wise for developing the computer program for turbidity data acquisition, Ms Michelle Lau for technical assistance and the CRC for Polymers for providing A.C.–H.C. with a CRC scholarship.

REFERENCES

1. Chan-Park, M. B. and McGarry, F. J., *J. Adv. Mat.*, 1995, **27**, 47.
2. Atkins, K. E., in *Sheet Moulding Compounds; Science and Technology*, ed. H. G. Kia, Hanser, Munich, 1993, Chapter 4.
3. Kinkelaar, M., Muzumdar, J. and Lee, L. J., *Polym. Eng. Sci.*, 1995, **35**, 823.
4. Huang, Y. -J. and Liang, C. -M., *Polymer*, 1996, **37**, 401.
5. Bucknall, C. B., Partridge, I. K. and Phillips, M. J., *Polymer*, 1991, **32**, 786.
6. Suspène, L., Yang, Y. S. and Pascault, J. -P., in *Toughened Plastics I*, ed. C. K. Riew and A. J. Kinloch, ACS, Washington, 1993, Chapter 7.
7. Pattison, V. A., Hindersinn, R. R. and Schwartz, W. T., *J. Appl. Polym. Sci.*, 1975, **19**, 3045.
8. Hsu, C. P., Kinkelaar, M. and Lee, L. J., *Polym. Eng. Sci.*, 1991, **31**, 1450.
9. Ruffier, M., Merle, G. and Pascault, J. P., *Polym. Eng. Sci.*, 1993, **35**, 466.
10. Suspène, L., Fourquier, D. and Yang, Y. -S., *Polymer*, 1991, **32**, 1593.
11. Williams, R. J. J., Rozenberg, B. and Pascault, J. -P., *Adv. Polym. Sci.*, 1997, **128**, 95.
12. Dusek, K., in *Developments in Polymerization—3*, ed. R. N. Haward, Applied Science Publishers, London, 1982, Chapter 4.
13. Kloosterboer, J. G., *Adv. Polym. Sci.*, 1998, **84**, 1.
14. Yang, Y. S. and Lee, L. J., *Polymer*, 1988, **28**, 1793.
15. Hsu, C. P. and Lee, L. J., *Polymer*, 1991, **32**, 2263; 1993, **34**, 4496, 4506, 4516.
16. Liu, S. B., Liu, J. L. and Yu, T. L., *J. Appl. Polym. Sci.*, 1994, **53**, 1165.
17. Bucknall, C. B., Davies, P. and Partidge, I. K., *Polymer*, 1985, **26**, 109.
18. Cook, W. D., Simon, G. P., Burchill, P. J., Lau, M. and Fitch, T. J., *J. Appl. Polym. Sci.*, 1997, **64**, 769.
19. Odian, G., *Principles of Polymerization*, 3rd edn, John Wiley, New York, 1991, Chapter 3.
20. Lem, K. -W. and Han, C. D., *Polym. Eng. Sci.*, 1984, **24**, 175.
21. Ozawa, T., *J. Therm. Anal.*, 1970, **2**, 301; 1975, **7**, 601.
22. ASTM E698-79, 1984.
23. Stannett, V. and Mesrobian, R. B., *J. Amer. Chem. Soc.*, 1950, **72**, 4125.
24. Brandrup, J. and Immergut, E. H., *Polymer Handbook*, 3rd edn, Wiley-Interscience, New York, 1989, II/40.
25. Soh, S. K. and Sunderberg, D. C., *J. Polym. Sci., Polym. Chem. Edn.*, 1982, **20**, 1299.
26. Stickler, M., *Macromol. Chem.*, 1983, **184**, 2563.
27. Burnett, G. M. and Cowley, P. R. E., *Trans. Far. Soc.*, 1953, **49**, 1490.
28. Kurland, J. J., *J. Polym. Sci., Polym. Chem. Ed.*, 1980, **18**, 1139.
29. Ramis, X. and Salla, J. M., *Polymer*, 1995, **36**, 3511.
30. Cook, W. D., *J. Appl. Polym. Sci.*, 1991, **42**, 2209.
31. McCrum, N. G., Read, B. E. and Williams, G., *Anelastic and Dielectric Effects in Polymeric Solids*, Dover Publications, New York, 1967, Chapter 9.
32. Flory, P. J., *Principles of Polymer science*, Cornell University Press, Ithaca, 1953, Chapter 11.